Reduction on Radiation Noise Level for Inductive Power Transfer Systems with Spread Spectrum focusing on Combined Impedance of Coils and Capacitors

Kent Inoue, Keisuke Kusaka, Jun-ichi Itoh
Nagaoka University of Technology
Department of Electrical, Electronics and Information
Nagaoka, Niigata, Japan
k_inoue@stn.nagaokaut.ac.jp, kusaka@vos.nagaokaut.ac.jp, itoh@vos.nagaokaut.ac.jp

***Abstract*—Two reduction methods on radiation noise of inductive power transfer (IPT) systems are proposed and experimentally demonstrated. In the IPT systems for electrical vehicles (EVs) or plug-in hybrid electrical vehicles (PHEVs), noise reduction technologies are strongly required because the radiation noise from the IPT system for EVs or PHEVs must not exceeds the limits on standards; for example the regulation by CISPR is well-known regulation. The proposed method suppresses the radiation noise using spread spectrum technique. The radiation noise from the transmission coils of the IPT system is spread in a frequency domain by changing the output frequency of an inverter at random. The output frequency is selected according to pseudo random numbers. The first proposed method; a spread spectrum with a uniform distribution (SSUD), evenly selects the output frequency within 80 kHz to 90 kHz. Another method; a spread spectrum with a biased distribution (SSBD) is focusing on the output current of the inverter. The possibility for the select of output frequency is biased in proportion to a combined impedance of the transmission coil and the resonance capacitors. In the experiments with an output power of 3 kW, the fundamental components are suppressed by 42.6% and 72.1% by applying the SSUD and the SSBD in comparison with the conventional system, which operates the inverter at a fixed frequency.**

Keywords—inductive power transfer; wireless power transfer; spread spectrum; random carrier; radiation noise; EMI

I. Introduction

In recent years, an IPT system are actively studied and developed [1–7]. Especially, a practical realization of the IPT systems for EVs or PHEVs is highly expected because the IPT system are capable to improve a usability of the EVs and PHEVs [8–13]. The IPT system transmits power using weak magnetic coupling between a primary coil and a secondary coil via large air-gap [14]. The fundamental principle of the IPT system is as same as a transformer. However, the weak coupling between the primary coil and the secondary coil such as 0.1–0.3 is specific characteristic of the IPT system.

In order to put the IPT system into a practical use, radiated electromagnetic noise have to be suppressed [15] to meet the standards (e.g. standard by CISPR is well-known regulation), because the IPT system never affects any wireless communication system, or electronic equipment.

One of the reduction methods on the noise is a use of filter circuit. A low-pass filter is connected to the input stage of the primary coil. The filter circuit suppresses the harmonics components of the current, which flows at the transmission coil. However, the radiation noise with a fundamental component cannot be suppressed. Moreover the power loss on the filter will increase because the cut-off frequency of the filter circuit has to be closed to the fundamental frequency. References [16–19] have proposed the suppression method using the magnetic shield or metal shield. The transmission coils are surrounded by plates made by magnetic material or metal. The radiation noise can be suppressed because these shields change a magnetic flux to an eddy current. However the eddy current increases the power loss of the IPT system. Besides, the aperture for magnetic path have to be ensured in the IPT system. Thus, the shielding provides the limited effect on the suppression of radiation noise. Ref. [20–21] have proposed the noise reduction method by forming the current, which flows in the coils, using the primary converter. However, the additional switches are required to reduce the radiation noise.

Incidentally, spread spectrum is widely used in a motor drive system with a PWM inverter [22–24]. This technique is also called as a random carrier PWM. The carrier frequency of the PWM inverter is constantly changed during the operation for the purpose of a reducing acoustic noise. By changing the carrier frequency, the frequency components of the acoustic noise caused by vibrations of windings is spread in a frequency domain [22–24]. The spread spectrum is also used in converters for the purpose of a reducing conducted electromagnetic interference (EMI) [25–27]. In both applications, the carrier frequency is changed to suppress the acoustic noise or electromagnetic noise. It means that the spread spectrum have not been applied to a square wave inverter. For this reason, the spectrum spread has not been applied to the IPT system because IPT system is generally driven by a square wave inverter.

In this paper, two reduction methods of the radiation noise for the IPT system based on a spread spectrum technique are proposed and demonstrated. The first proposed method; spread spectrum with uniform distribution (SSUD), suppress the radiation noise using a spread spectrum. In this method, the output frequency is selected from a uniform probability distribution. The second method; spread spectrum with biased distribution (SSBD), selects the output frequency from a biased probability distribution. The probability distribution is proportional to the combined impedance of a compensation capacitor and a transmission coil. In the rest of the papers, first, the regulations on electromagnetic noise for the IPT system is shown. Then, two proposed methods are explained in the chapter 3. In the chapter 4, the proposed methods are implemented into the prototype with an output power of 3 kW. Finally, the effect on the system efficiency is evaluated.

II. Allowable Radiation Noise Level in Japan

Figure 1 shows the regulations of the radiation noise in Japan for IPT systems with an output power of 7 kW or less [28]. Note that the regulations are under discussion in Japan for the standardization. In Japan, a use of a frequency range from 79 kHz to 90 kHz is considered for an IPT system of EVs. This regulation is basically conformed to the CISPR11 Group 2, Class B [29]. However the limits of the radiation noise within 79 kHz to 90 kHz will be mitigated to 68.4 dBμA/m. Moreover, the limits on the following frequency bands will be mitigated by 10 dB.

- 158 kHz – 180 kHz
- 237 kHz – 270 kHz
- 316 kHz – 360 kHz
- 395 kHz – 450 kHz

Besides, in the IPT system, the allowable limits within 9 kHz to 150 kHz is added. The radiation noise on the frequency band except the band within 79 kHz to 90 kHz have to be lower than 23.1 dBμA/m. Similarly, the allowable limits on the frequency within 526.5 kHz to 1606.5 kHz is −2.0 dBμA/m because this frequency band have been used for amplitude modulation (AM) broadcasting.

Note that, CISPR11 prescripts to measure the noise using a quasi-peak measuring method. From the regulations, the frequency components on the radiation noise should be suppressed not only the fundamental component but also the harmonics component.

III. Proposed Noise Reduction Methods

A. Compensation Circuits

Figure 2 shows the typical circuit configuration of the IPT system with a series–series compensation (S/S) [30]. In the IPT system for EVs, primary coils are buried in roads or parking. In contrast, secondary coils are beneath the bottom of the cars. For this reason, magnetic coupling between the primary coil and the secondary coil is weak. The large leakage inductance attributed to the weak magnetic coupling causes an increase of reactive power. In order to solve above problems, the compensation circuits such as a series–series compensation (S/S), a series–parallel compensation (S/P) are widely used in order to cancel out the leakage inductance [31].

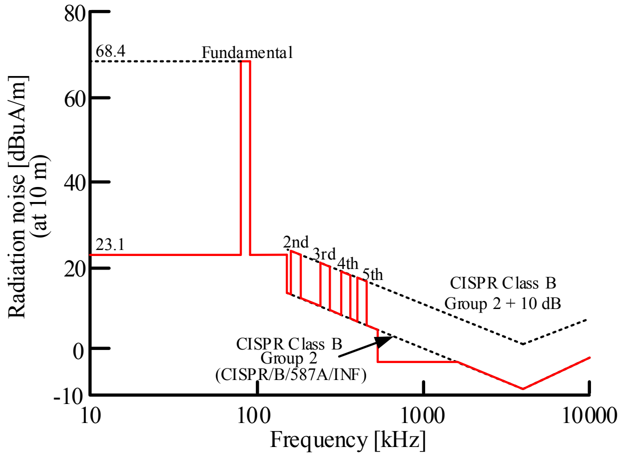

Fig. 1. Allowable limits on radiation noise of 7-kW or less IPT system for EVs in Japan (under discussion).

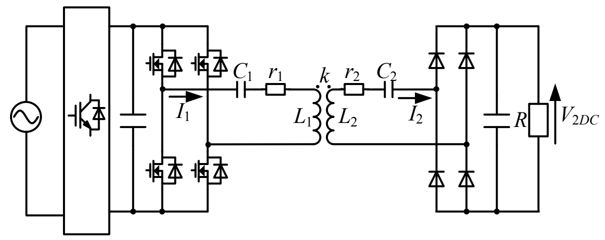

Fig. 2. Typical system configuration of IPT system for EVs.

The primary current and the secondary current are calculated as (1) and (2) when an input voltage V_1 is applied into the primary side. Note that the voltage V_1 is the fundamental component of the output voltage of the inverter.

$$\dot{I}_1 = \frac{r_2 + R_{eq} + j\left(\omega L_2 - \frac{1}{\omega C_2}\right)}{\left\{r_1 + j\left(\omega L_1 - \frac{1}{\omega C_1}\right)\right\}\left\{r_2 + R_{eq} + j\left(\omega L_2 - \frac{1}{\omega C_2}\right)\right\} + \omega^2 L_m^2}\dot{V}_1 \quad (1)$$

$$\dot{I}_2 = \frac{j\omega L_m}{\left\{r_1 + j\left(\omega L_1 - \frac{1}{\omega C_1}\right)\right\}\left\{r_2 + R_{eq} + j\left(\omega L_2 - \frac{1}{\omega C_2}\right)\right\} + \omega^2 L_m^2}\dot{V}_1 \quad (2)$$

where R_{eq} is the equivalent load considering the rectifier, r_1 is the equivalent series resistance of the primary winding, r_2 is the equivalent series resistance of the secondary winding, L_1 is the primary inductance, L_2 is the secondary inductance, C_1 is the primary compensation capacitor, C_2 is the secondary compensation capacitor, L_m is the mutual inductance and ω is the angular frequency of the power supply. The equivalent load is expressed by (3) using the analysis given in [30].

$$R_{eq} = \frac{8}{\pi^2}\frac{V_{2DC}^2}{P_2} \tag{3}$$

where V_{2DC} is the secondary DC voltage and P_2 is the output power.

The compensation capacitors are generally selected to cancel out the reactive power at the input frequency. Thus, the compensation capacitors can be calculated by (4) and (5).

$$C_1 = \frac{1}{L_1\omega^2} \tag{4}$$

$$C_2 = \frac{1}{L_2\omega^2} \tag{5}$$

The primary current with the compensation is expressed by

$$\dot{I}_1 = \frac{r_2 + R_{eq}}{r_1\left(r_2 + R_{eq}\right) + \omega^2 L_m^2}\dot{V}_1 \tag{6}.$$

Due to the compensation circuit, the input impedance from the view point of the output of the power supply is relatively low. Thus the input current contains large fundamental component. Note that, the input current contains the low-order harmonic components depending on the coupling between the primary and the secondary coils.

The radiation noise is mainly caused by the current, which flows in the primary coil and the secondary coil. For other converters, the shielding with magnetic material and metal are effective to suppress radiated noise. However, in the IPT system, the aperture for magnetic path have to be ensured. Thus, the shielding provides the limited effect on the suppression of radiation noise.

B. Proposed Noise Reduction Method

In this paper, the radiation noise is spread in a frequency domain by changing the output frequency of the voltage-source inverter in two manners. The output frequency is selected at random within 80 kHz to 90 kHz. In the SSUD, the output frequency is selected from a discrete uniform probability distribution. By selecting the output frequency of the voltage source inverter from the uniform distribution, the harmonics components of the voltage is evenly spread. On the other hand, SSBD selects the output frequency of the voltage source inverter from a biased probability distribution. The probability distribution is biased to be proportional to a combined impedance of the transmission coil and the compensation capacitor. Due to the biased probability distribution, the harmonic components of the current, which is output from the inverter, is spread. The spread spectrum increases the reactive current in comparison with the operation under the resonance condition. However, the decrease of noise by the spread spectrum is larger than the increase of noise caused by the reactive current.

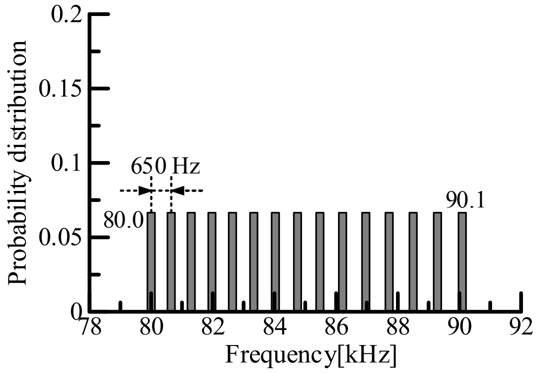

(a) Proposed method I: spread spectrum with uniform distribution (SSUD)

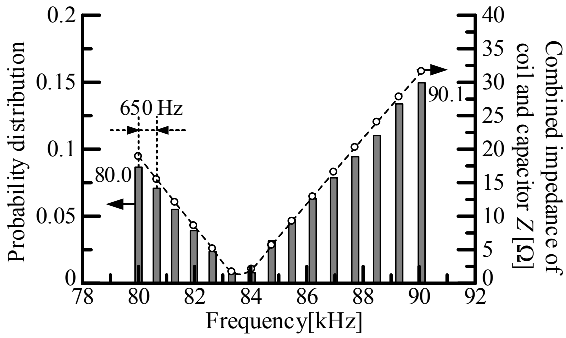

(b) Proposed method II: spread spectrum with biased distribution (SSBD)

Fig. 3. Probability distributions for spread spectrum.

Figure 3 shows the probability distribution of the output frequency of the inverter. Fig. 3 (a) is the probability distribution of SSUD. The probability distribution is discrete uniform distribution within 80 kHz to 90 kHz. It means that the each output frequency is evenly selected. Note that, the parameter is discrete because the carrier for the inverter is generated in the FPGA. The output frequency is renewed at every periods. By selecting the output frequency of the voltage source inverter from the uniform distribution, the harmonics components of the voltage is evenly spread. Fig. 3 (b) is the probability distribution of SSBD. In the IPT system, the input impedance of the IPT system depends on the frequency. Thus the probability distribution is proportional to the combined impedance of the coil and the compensation capacitor. By selecting the output frequency of the voltage source inverter from the biased distribution, the harmonics components of the current is evenly spread.

Table I shows the assignment of the pseudo random numbers for the output frequency. Table I (a) is for the proposed method focusing on the inverter output voltage. Table I (b) is for the

TABLE I. ASSIGNMENT OF OUTPUT FREQUENCY

(a) For proposed method I: SSUD

	Psuedo random number	Frequency [kHz]		Psuedo random number	Frequency [kHz]
1	0000001	80.00	65	1000001	85.47
⋮	⋮	80.00	⋮	⋮	85.47
8	0001000	80.00	72	1001000	85.47
9	0001001	80.65	73	1001001	86.21
⋮	⋮	80.65	⋮	⋮	86.21
16	0010000	80.65	80	1010000	86.21
17	0010001	81.30	81	1010001	86.96
⋮	⋮	81.30	⋮	⋮	86.96
24	0011000	81.30	88	1011000	86.96
25	0011001	81.97	89	1011001	87.72
⋮	⋮	81.97	⋮	⋮	87.72
32	0100000	81.97	96	1100000	87.72
33	0100001	82.64	97	1100001	88.50
⋮	⋮	82.64	⋮	⋮	88.50
40	0101000	82.64	104	1101000	88.50
41	0101001	83.33	105	1101001	89.29
⋮	⋮	83.33	⋮	⋮	89.29
48	0110000	83.33	112	1110000	89.29
49	0110001	84.03	113	1110001	90.09
⋮	⋮	84.03	⋮	⋮	90.09
56	0111000	84.03	120	1111000	90.09
57	0111001	84.75			
⋮	⋮	84.75			
64	1000000	84.75			

(b) For proposed method II: SSBD

	Psuedo random number	Frequency [kHz]		Psuedo random number	Frequency [kHz]
1	0000001	80.00	42	0101010	85.47
⋮	⋮	80.00	⋮	⋮	85.47
11	0001011	80.00	47	0101111	85.47
12	0001100	80.65	48	0110000	86.21
⋮	⋮	80.65	⋮	⋮	86.21
20	0010100	80.65	55	0110111	86.21
21	0010101	81.30	56	0111000	86.96
⋮	⋮	81.30	⋮	⋮	86.96
27	0011011	81.30	65	1000001	86.96
28	0011100	81.97	66	1000010	87.72
⋮	⋮	81.97	⋮	⋮	87.72
32	0100000	81.97	77	1001101	87.72
33	0100001	82.64	78	1001110	88.50
⋮	⋮	82.64	⋮	⋮	88.50
35	0100011	82.64	91	1011011	88.50
36	0100100	83.33	92	1011100	89.29
37	0100101	84.03	⋮	⋮	89.29
38	0100110	84.75	108	1101100	89.29
⋮	⋮	84.75	109	1101101	90.09
41	0101001	84.75	⋮	⋮	90.09
			127	1111111	90.09

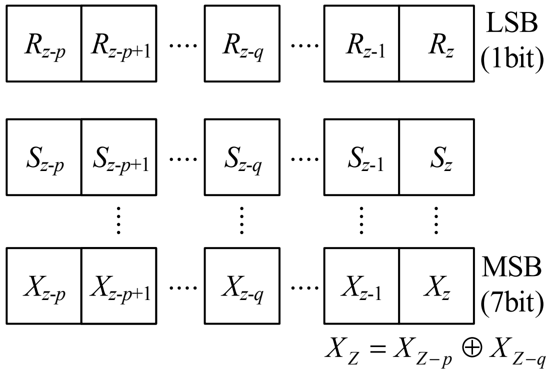

Fig. 4. Generation method of 7-bit pseudo random numbers based on a maximal length sequence.

proposed method focusing on the inverter output current. The output frequency is selected according to generated 7-bit pseudo random numbers.

Figure 4 shows the generation method of pseudo random numbers. The pseudo random numbers are generated using a maximal length sequence (M-sequence) [25] [32] in the DSP. Note that, the different pseudo random number generation methods can be used. However the generation method using an M-sequence is chosen in this paper because a complex generation method of a pseudo random number is not suitable for an implementation of an algorithm for the DSP. An M-sequence random number is generated by (7).

$$X_Z = X_{Z-p} \oplus X_{Z-q} \tag{7}$$

where $X_{z\text{-}p}$ and $X_{z\text{-}q}$ are the present value X_Z delayed by p period and q period, respectively ($p > q$). In this paper, $p = 7$, $q = 1$ are used. Moreover, the number of bits of pseudo random number is seven. The pseudo random number is calculated by an exclusive or of the $X_{Z\text{-}p}$ and $X_{Z\text{-}q}$.

IV. Experimental Results

A. Experimental Setup

Figure 5 and Table II show the configuration for the prototype and the specifications, respectively. In this experiments, the 420-V DC voltage power supply is used. As switching devices, silicon-carbide (SiC) MOSFETs and SiC diodes are used. The SiC- MOSFETs are controlled by the FPGA and the DSP.

The inductances of the primary coil and the secondary coil are designed according to the following equation [12] assuming the effect of the spread spectrum can be ignored where ω_0 is the center frequency of the frequency range, which is used for the spread spectrum.

$$L_1 = \frac{R_{eq}}{\omega_0 k_0} \frac{V_{1DC}^2}{V_{2DC}^2} \quad (8)$$

$$L_2 = \frac{R_{eq}}{\omega_0 k_0} \quad (9)$$

The compensation circuit can be calculated by (4) and (5) using the center frequency ω_0. It means that the resonance circuit is designed to resonate at 85.1 kHz.

Figure 6 shows the primary coil and the secondary coil for the prototype. Solenoid-type coils [33] are used as the transmission coils. Note that the transmission distance is 150 mm assuming the transmission from a road to a bottom of the EVs or PHEVs.

B. *Operation Waveforms*

Figure 7 shows the operation waveforms. In the all of the operation methods, the output power is 3 kW. Fig. 7 (a) is the waveforms with a conventional method. The output frequency is fixed at 85.1 kHz. Fig. 7 (b) is the waveforms with SSUD. The output frequency of the voltage source inverter is selected according to Table I (a) at random. Fig. 7 (c) is the waveforms with SSBD. The output frequency is selected according to Table I (b). In Fig. 7 (b) and (c), the output frequency is changed within 80 kHz to 90 kHz in every periods according to pseudo random numbers. When the proposed methods are applied, the amplitudes of the primary current i_1 varies. However, the constant output voltages are obtained in spite of the operation methods.

C. *Harmonics Components Analysis*

Figure 8 shows the harmonics components of the primary current i_1. Fig. 8 (a) is the result with the conventional method. Fig. 8 (b) and (c) are the results with the proposed methods; SSUD and SSBD, respectively. The lower figures shows the results focusing on the fundamental components. In this paper, the harmonics components of the primary current are evaluated instead of the radiation noise because the radiation noise from a loop coil is proportional to the amplitude of current. When the conventional method is used, the fundamental component and low-order harmonics components sharply appear. In contrast, when the proposed method is used, the maximum value on the fundamental and low-order harmonics are suppressed. The harmonics components around the fundamental frequency is suppressed by 42.6% and 72.1% by using the SSUD and SSBD in comparison with the conventional method, which operates the inverter at fixed frequency. In same manner, the low-order harmonic components are suppressed in comparison with the conventional system. Both the proposed methods are valid to suppress the components. In the operation with SSUD, however, harmonics components peak at 85.1 kHz. It is caused by the frequency characteristic of the IPT system. In the IPT system the impedance from the view point of the power supply takes minimum value at the resonance angular frequency ω_0. Thus, the current harmonics has peak at the resonance angular frequency

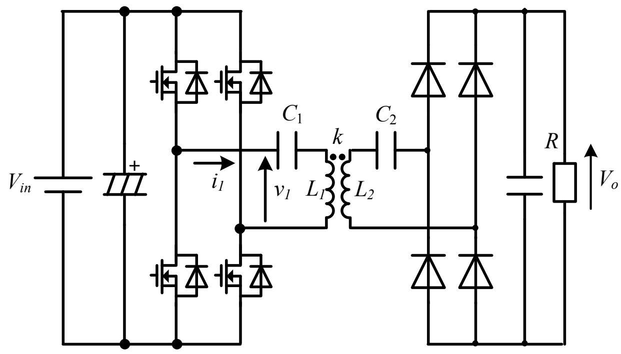

Fig. 5. Experimental setup.

TABLE II. SPECIFICATIONS OF PROTOTYPE.

	Symbol	Value
Input DC voltage	V_{in}	420 V
Coupling coefficient	k	0.2
Primary inductance	L_1	392 uH
Secondary inductance	L_2	401 uH
Primary capacitance	C_1	8.96 nF
Secondary capacitance	C_2	8.78 nF
Transmission distance	l	150 mm
MOSFETs	SCH2080KEC (Rohm)	
Diodes	SCS220AE (Rohm)	
Ferrite plates	PC40 (TDK)	

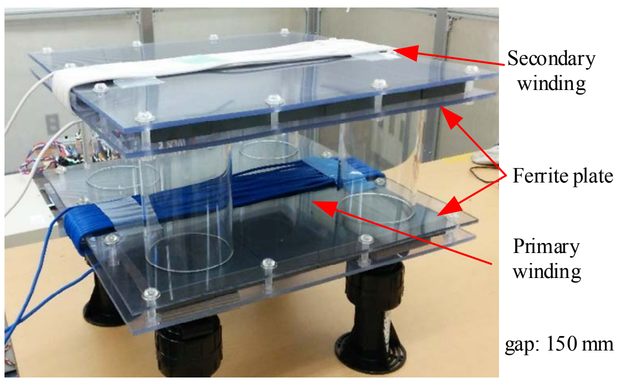

Fig. 6. Transmission coils with a rated power of 3 kW. The solenoid type is chosen.

even if the output frequency of the voltage is spread in the frequency domain.

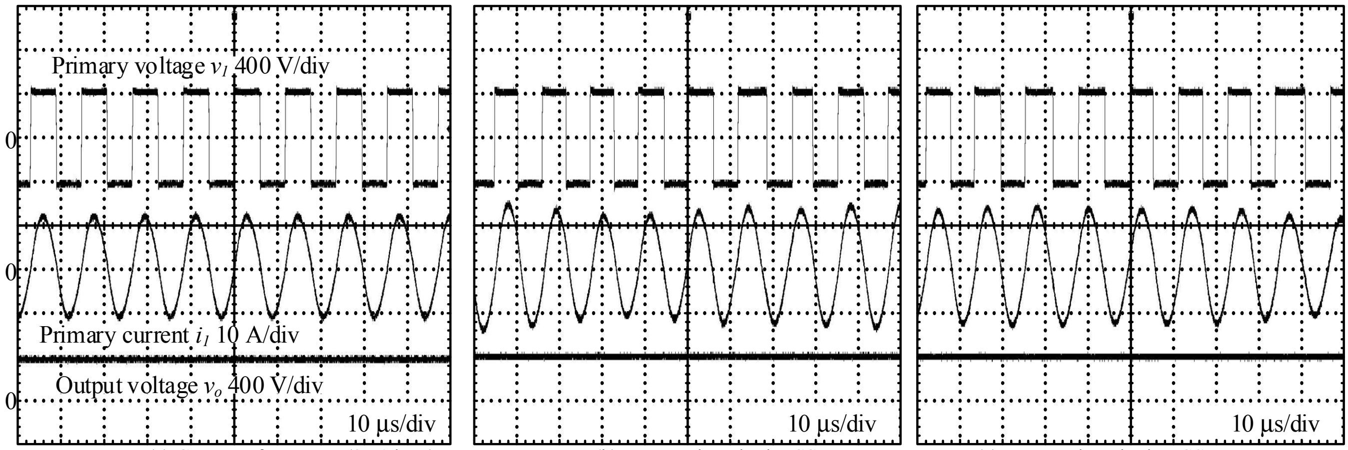

(a) Constant frequency (85.1 kHz) (b) Proposed method I: SSUD (c) Proposed method II: SSBD

Fig. 7. Operation waveforms of IPT system.

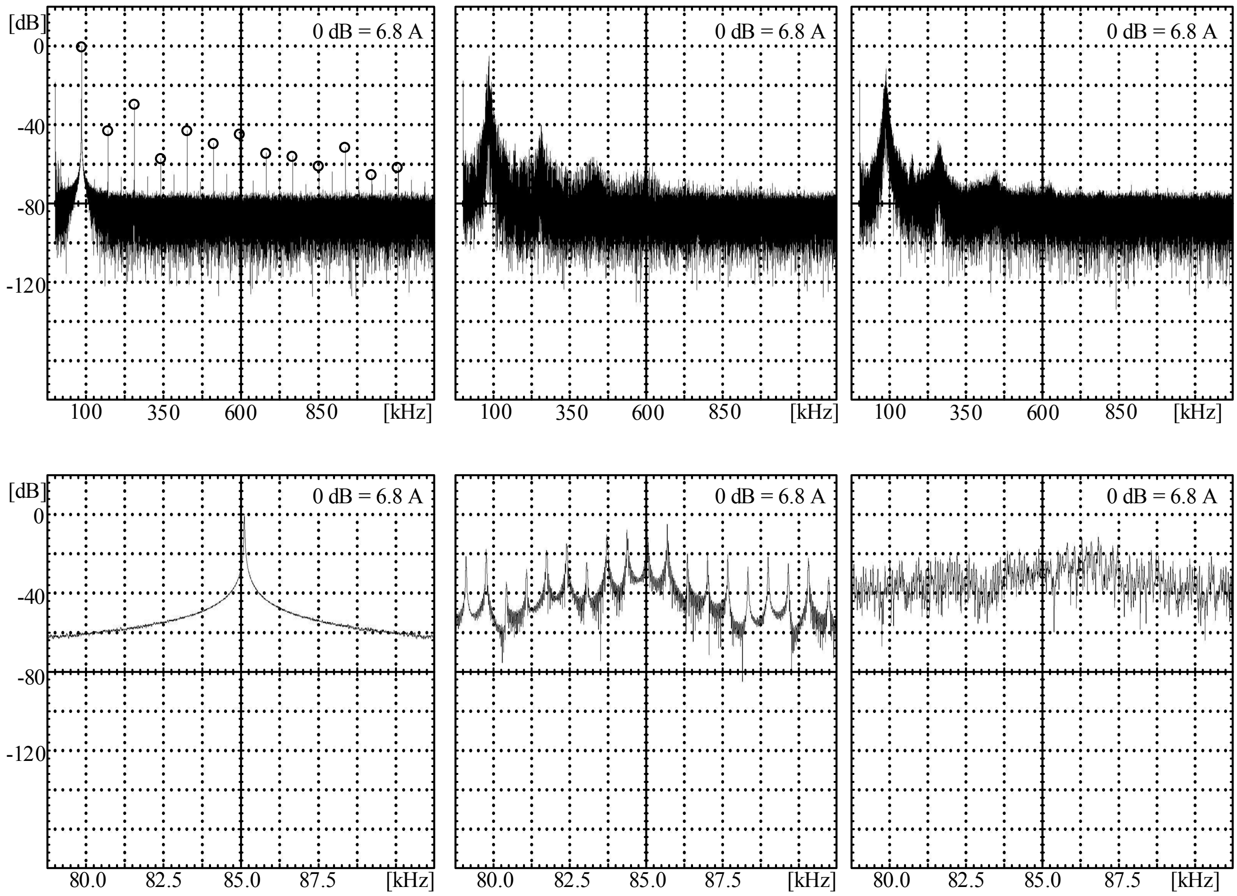

(a) Constant frequency (85.1 kHz) (b) Proposed method I: SSUD (c) Proposed method II: SSBD

Fig. 8. Harmonics components on the prmary current.

D. Efficiency Evaluation

Figure 9 shows the DC-to-DC efficiency characteristics. Note that the efficiency is defined as the ratio of the input DC power to the output DC power. All of the curves show similar characteristics. The maximum efficiency is 94.9% at an output power of 3.0 kW when the inverter is operated at fixed frequency. In contrast, the maximum efficiency is 94.1% at an output power of 3.0 kW when the SSUD is used. The decrease of efficiency is attributed to the increased reactive current due to the difference between the operating frequency and the resonance frequency. The reactive current increases the copper loss, iron loss, conduction loss and switching loss on the converter. However, the decrease in an efficiency is 0.78%. When the SSBD is used, the maximum efficiency is 93.8% at an output power of 3.0 kW. The decrease in the efficiency is 1.1% in comparison with the conventional method. Thus SSBD is effective in the heavy-load region. In contrast, the efficiency drops by 4.4% at a maximum, when an output power is 1.0 kW. In the light-load region, the effect of the no-load loss is relatively larger in comparison with the effect in the heavy-load. However, the current in windings is relatively smaller than the current with the heavy load. Considering that the radiation noise is proportional to the current, in the light-load region, the weak effect on the suppression of the radiation noise can be acceptable. In the light-load region, therefore, SSUD should be used.

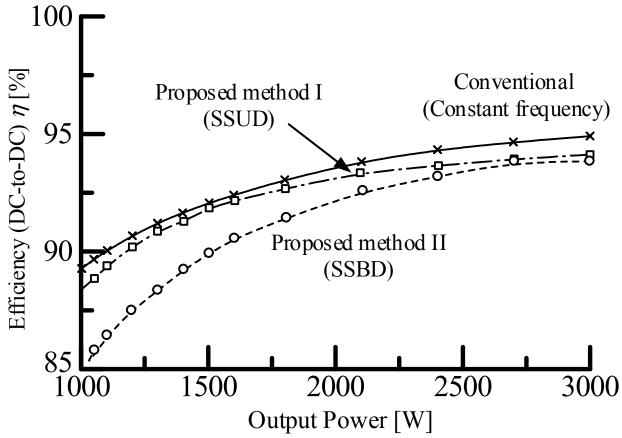

Fig. 9. Efficiency characteristics.

V. CONCLUSION

In this paper, two reduction methods on radiation noise of the inductive power transfer system are proposed and experimentally demonstrated. The radiation noise from the transmission coils for an IPT system is spread in a frequency domain by changing the output frequency of the voltage source inverter at random. Therefore, additional components such as a noise shield and a filter circuit are not required in the proposed methods. The first proposed method; spread spectrum with uniform distribution (SSUD) selects the output frequency of the voltage source inverter within 80 kHz to 90 kHz from the discrete uniform probability distribution. The second proposed; spread spectrum with biased distribution (SSBD), selects the output frequency from the biased discrete probability distribution. The probability distribution is proportional to the combined impedance of the transmission coil and the compensation capacitor considering the frequency characteristic of the IPT system. Owing to the bias, the frequency components of the output current, which flows in the transmission coils, is even within 80 kHz to 90 kHz. From the experimental results with an output power of 3.0 kW, the primary current around a fundamental component are suppressed by 42.6% and 72.1% by applying the SSUD and SSBD, respectively. Therefore SSBD is more effective to suppress the noise than SSUD and the conventional method unless it works in the light-load region. In the light-load region, SSUD may increase the no-load loss, which dominates the loss. Therefore, SSUD should be used in the light-load region.

REFERENCES

[1] S. Y. R. Hui, W. Zhong, C. K. Lee: "A Critical Review of Recent Progress in Mid-Range Wireless Power Transfer", IEEE Trans. On Power Electronics, Vol. 29, No. 9, pp. 4500-4511 (2014)

[2] D. Shimode, T. Mura, S. Fujiwara, "A Study of Structure of Inductive Power Transfer Coil for Railway Vehicles," IEEJ Journal of Industry Applications, Vol. 4, No. 5, pp. 550-558 (2015)

[3] Y. Hayashi, Y. Chiku, "Contactless DC Connector Concept for High-Power –Density 380-V DC Distribution System," IEEJ Journal of Industry Applications, Vol. 4, No. 1, pp. 49-58 (2015)

[4] K. Kusaka, K.Orikawa, J. Itoh, I. Hasegawa, K. Morita, T. Kondo, "Galvanic Isolation System with Wireless Power Transfer for Multiple Gate Driver Supplies of a Medium-voltage Inverter," IEEJ Journal of Industry Applications, Vol. 5, No. 3, pp. 206-214 (2016)

[5] T. Mizuno, T. Ueda, S. Yashi, R. Ohtomo, Y. Goto, "Dependence of Efficiency on Wire Type and Number of strands of Litz Wire for Wireless Power Transfer of Magnetic Resonant Coupling," IEEJ Journal of Industry Applications, Vol. 3, No. 1, pp. 35-40 (2014)

[6] N. K. Trung, T. Ogata, S. Tanaka, K. Akatsu, "Analysis and PCB Design of Class D Inverter for Wireless Power Transfer Systems Operating a 13.5 MHz," IEEJ Journal of Industry Applications, Vol. 4, No. 6, pp. 703-713 (2015)

[7] J. T. Boys, G. A. Covic, Y. Xu: "DC Analysis Technique for Inductive Power Transfer Pick-Ups," IEEE Trans. On Power Electronics, Vol. 1, No. 2, pp. 51-53 (2003)

[8] Siqi Li, Chunting C. Mi: "Wireless Power Transfer for Electric Vehicle Applications", IEEE Journal, Vol.3, No.1, pp.4-17 (2015)

[9] S. Li, C. C. Mi: "Wireless Power Transfer for Electric Vehicle Applications," IEEE Journal of Emerging and Selected Topics in Power Electronics, Vol. 3, No. 1, pp. 4-17 (2015)

[10] T. Shijo, K. Ogawa, S. Obayashi: "Optimization of Thickness and Shape of Core Block in Resonator for 7 kW-Class Wireless Power Transfer," IEEE Energy Conversion Congress and Exposition 2015, pp. 3099-3102 (2015)

[11] R. Ota, N. Hoshi, J. Haruna, "Design of Compensation Capacitor in S/P Topology of Inductive Power Transfer System with Buck or Boost Converter on Secondary Side," IEEJ Journal of Industry Applications , Vol. 4. No. 4, pp. 476-485 (2015)

[12] R. Bosshard, J. W. Kolar, J. Muhlethaler, I. Stevanovic, B. Wunsch, F. Canales: "Modeling and eta-alpha-Pareto Optimization of Inductive Power Transfer Coils for Electric Vehicles", IEEE Journal of Emerging and Selected Topics in Power Electronics, Vol. 3, No. 1, pp. 50-64 (2015)

[13] R. Haldi, K. Schenk: "A 3.5 kW Wireless Charger for Electric Vehicles with Ultra High Efficiency", IEEE Energy Conversion Congress & Expo 2014, pp. 668-674 (2014)

[14] T. Imura, Y. Hori: "Maximizing Air Gap and Efficiency of Magnetic Resonant Coupling for Wireless Power Transfer Using equivalent Circuit and Neumann Formula," IEEE Trans. On Industrial Electronics, Vol. 58, No. 10, pp. 4746-4752 (2011)

[15] J. Kim, H. Kim, M. Kim, S. Ahn, J. Kim, J. Kim: "Analysis of EMF Noise from the Receiving Coil Topologies for Wireless Power Transfer", Asia-Pacific Symposium on Electromagnetic Compatibility (APEMC) 2012 , pp.645-648 (2012)

[16] M. Jo, Y. Sato, Y. Kaneko, S. Abe: "Methods for Reducing Leakage Electric Field of a Wireless Power Transfer System for Electric Vehicles", ECCE US, pp.1762-1769 (2014)

[17] H. Kim, J. Cho, S. Ahn, J. Kim, J. Kim: "Suppression of Leakage Magnetic Field from a Wireless Power Transfer System using Ferrimagnetic Material and Metallic Shielding," IEEE International Symposium on EMC, 978-1-4673-2061-0, pp.640-645 (2012)

[18] T. Campi, S. Cruciani, M. Feliziani: “Magnetic Shielding of Wireless Power Transfer Systems,” IEEE International Symposium on EMC, 15A-H1, pp.422-425 (2014)

[19] K. Maikawa, K. Imai, Y. Minagawa, M. Arimitsu, H. Iwao: “Magnetic Field Reduction Technology of Wireless Charging System,” in Proceedings, Society of Automotive Engineers of Japan 2013, No. 110-13 (2013)

[20] K. Kusaka, J. Itoh: “A Suppression Method of Radiated Emission caused by Low-order Harmonic Current in a Wireless Power transfer System,” IEE of Japan Annual meeting 2015, No. 4-117, pp. 196-197 (2015) (in Japanese)

[21] D. Narita, T. Imura, H. Fujimoto, Y. Hori: “Electromagnetic Field Suppression in Polyphase Wireless Power Transfer via Magnetic Resonance Coupling”, Technical report of IEICE, No. WPT2014-31, pp.39-44 (2014) (in Japanese)

[22] A. M. Trzynadlowski, F. Blaabjerg, J. K. Pedersen, R. L. Kirlin, S. Legowski, “Random Pulse Width Modulation Techniques for Converter-Fed Drive Systems – A Review,” IEEE Trans. On Industry Applications, Vol. 30, No. 5, pp. 1166-1175 (1994)

[23] J. T. Boys, P. G. Handley, “Spread spectrum switching: low noise modulation technique for PWM inverter drives,” IEEE Proceedings B – Electric Power Application, Vol. 139, No. 3, pp. 252-260 (1992)

[24] C. M. Liaw, Y. M. Lin, C. H. Wu, K. I. Hwu, ”Analysis, Design, and Implementation of a Random Frequency PWM Inverter,” IEEE Trans. On Power Electronics, Vol. 15, No. 5, pp. 843-854

[25] K. Kim, Y. Jung, Y. Lim, “A New Hybrid Random PWM Scheme,” IEEE Trans. on Power Electronics, Vol. 24, No. 1. pp. 192- 200 (2009)

[26] K. K. Tse, H. S. Chung, S. Y. Hui, H. C. So, “Analysis and Spectral Characteristics of a Spread-Spectrum Technique for Conducted EMI Suppression,” IEEE Trans. On Power Electronics, Vol. 15, No. 2. pp. 399-410 (2000)

[27] D. Stone, B. Chambers, D. Howe, “Random Carrier Frequency Modulation of PWM Waveforms to Ease EMC Problems in Switched Mode Power Supplies,” International Conference on Power Electronics and Drive Systems 1995, pp. 16-21 (1995)

[28] Ministry of Internal Affairs and Communications, Japan, “Inquary of technical requirements for wireless power transfer system for EVs in technical requirements for wireless power transfer system in standards of International Special Committee on Radio Interference (CISPR),” No. 3 (2015) (in Japanese)

[29] CISPR 11: 2015, “Industrial, scientific and medical equipment – Radio-frequency disturbance characteristics – Limits and methods of measurement (2015)

[30] Y. H. Sohn, B. H. Choi, E. S. Lee, G. C. Lim, G. Cho, C. T. Rim: "General Unified Analyses of Two-Capacitor Inductive Power Transfer Systems: Equivalence of Current-Source SS and SP Compensations", IEEE Trans. On Power Electronics, Vol. 30, No. 11, pp. 6030-6045 (2015)

[31] R. L. Steigerwald, “A Comparison of Half-Bridge Resonant Converter Topologies,” IEEE Trans. on Power Electronics Vol. 3, No. 2, pp. 174-182 (1992)

[32] F. J. MacWilliams, N. J. A. Sloane, “Pseudo-random sequences and arrays,” Proceedings of the IEEE, Vol. 64, No. 12, pp. 1715-1729 (1976)

[33] G. A. Covic, J. T. Boys, “Modern Trends in Inductive Power Transfer for Transportation Application,” IEEE Journal of Emergin and Selected Topics in Power Electronics, Vol. 1, No. 1. pp. 28-41 (2013)